

# Contribution to the optimization of the physical layer of 5G mobile systems by improving the performance of FBMC-OQAM modulation

THEODORET Nosisoa<sup>1</sup>, RANDRIAMITANTSOA Paul Auguste<sup>2</sup>

<sup>1</sup> PhD student, TASI, ED-STII, Antananarivo, Madagascar

<sup>2</sup> Thesis director, TASI, ED-STII, Antananarivo, Madagascar

## ABSTRACT

User expectations are becoming more pressing in terms of transmission rate and acceptable latency. The deployment of the 5G will provide a reliable network with consistent performance and heterogeneous service qualities according to the needs of users regardless of their position relative to the base station. In the real world, the performance of the transmission system depends on the characteristics of the propagation channel (flat channel or selective channel) and the profile of the users who are classified according to their mobility speed. Depending on the needs of the users, the designers must take into account several factors such as the speed of data transfer (latency), the ability to receive reliable information (low bit error rate) despite the extreme transmission conditions (speed up to 500 km / h). Multicarrier modulations are able to accommodate multiple paths limiting the performance of digital transmissions. The success of OFDM modulation lies in its ability to resist selective channel fading and intersymbol interference. However, some of the characteristics of OFDM systems, such as poor frequency localization and extremely high PAPR, limit their operation by 5G systems that aim to meet users' requirements in terms of data rates, spectral efficiency, energy efficiency and latency. . Thus, it is essential to find an alternative modulation scheme that will be able to support several scenarios related to the technical specifications of 5G.

**Keyword:** 5G, FBMC-OQAM, SIR, power spectral density, PAPR

## 1. INTRODUCTION

From a theoretical point of view, this article establishes a new research framework based on the profile of FBMC-OQAM multicarrier modulations that are close to the technological requirements imposed by 5G networks despite pressure from some operators to support maintaining the adoption of OFDM modulations. [1] [2] [3]

To validate our theoretical hypotheses, a test bench has been developed to support the three scenarios mentioned below. It is a near-real-time measurement tool since the signal is generated offline and then transmitted over a wireless channel and ultimately evaluated offline, allowing large-scale network performance to be assessed through Monte Carlo simulations.

The scenarios we have implemented are:

- A scenario in which critical communications involve transmission is low latency and very high reliability: to reduce the latency and ensure the coexistence of different types of services, we will use different frequency subspaces for each requested service. Thus, some frequency resources may be used for MBB (Mobile Broadband) services and adjacent frequencies may be used for Mission Critical Communications (MCC) services.

- A scenario to determine the uplink access technique compatible with the 3 generic services of 5G: it will be question of proposing an access technique to extend the life of sensor batteries and ensure reliable communication in extreme transmission conditions.

### 1.1 Block diagram of the OFDM modulation

Multicarrier modulation techniques effectively combat selective channel fading and intersymbol interference. Through frequency multiplexing, the data is distributed simultaneously over a large number of carriers. In the frequency domain, the bandwidth is designed to be smaller than the coherency bandwidth and each sub-channel can be considered a flat fading channel.

In the time domain, by dividing the high-speed data stream into a number of low-rate data streams and transmitted in parallel, the problem of intersymbol interference is solved. OFDM techniques bring a clear improvement to conventional multicarrier modulations. Indeed, the OFDM system uses orthogonal subcarriers to allow a spectral overlap and to optimize the spectral efficiency.

One of the characteristics of the OFDM systems is the orthogonality condition which is essential to ensure that there is no interference between the carriers. From a frequency point of view, the orthogonality condition can be defined by the choice of the difference between the carriers. The frequencies are orthogonal if the space between two adjacent frequencies is equal  $\frac{1}{T_0}$ . Each carrier modulates a symbol during a time rectangular window of duration  $T_0$

and its spectrum in frequency is a cardinal sinus which vanishes all the multiples of  $\frac{1}{T_0}$ .

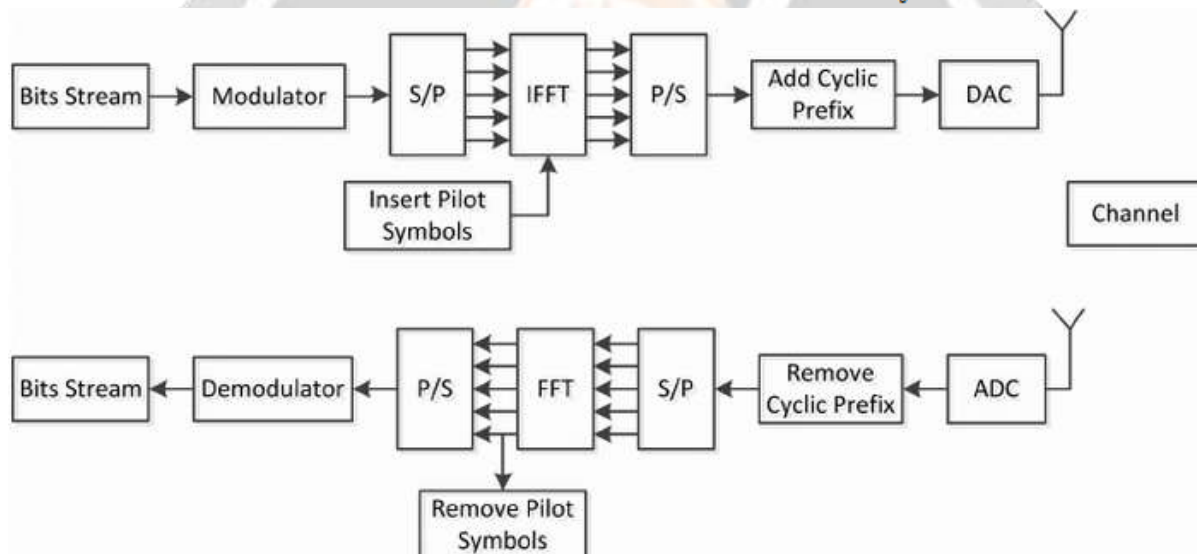


Fig -1: Block Diagram of OFDM Transmission System

F-OFDM modulation differs from OFDM modulation in the following properties: [7]

- The band can be divided into several sub-bands but each of the sub-bands can have a different bandwidth.
- Each sub-band is composed of several subcarriers but the spacing between the subcarriers may differ from one sub-band to another.

WOLA modulation is an improvement in OFDM modulation by applying an overlap method and a windowing operation on each OFDM symbol in the time domain. To compensate for the overlap effect, the cyclic prefix is extended. The shape of the window is based on the RRC function, so that the consecutive WOLA symbols overlap in the time domain. If the OFDM modulation uses a rectangular pulse prototype filter, the WOLA modulation applies a window that smooths the edges of the rectangular pulse, in order to improve spectrum utilization. [6]

The windowing function is a pulse function with fuzzy edges on both sides, so that the length of the window is extended to  $\left[-\frac{L_{wrt}}{2}, N + \frac{L_{wrt}}{2}\right]$  where  $L_{wrt}$  is the length of the extension beyond the length of the cyclic prefix. The fuzzy edges at the beginning and end of the windowing function will result in better localization of the WOLA waveform in the frequency domain.

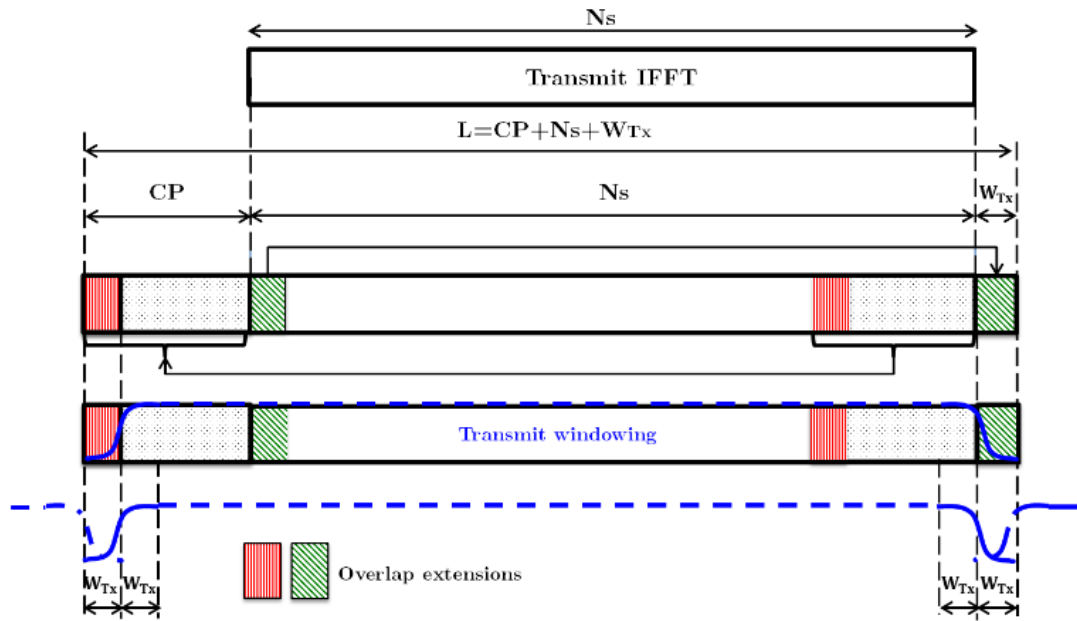


Fig -2: WOLA processing: Transmitter side

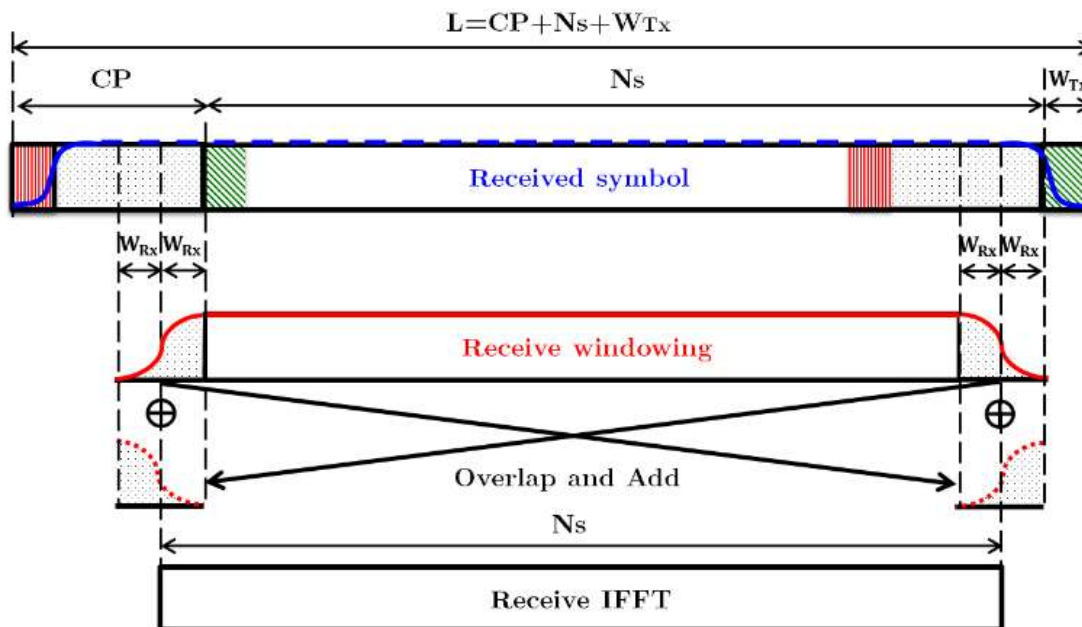


Fig -3: WOLA processing: Receiver side

**1.2 Block diagram of FBMC-OQAM modulation**

For the FBMC-OQAM technique, prototype filters with overlapping impulse responses that meet the Nyquist criterion are applied.

The overlap factor  $K$  is a parameter used to define the number of overlapping symbols and corresponds to the ratio between the length of the filter  $L$  and the total number of subcarriers  $M$ .

The transmitted FBMC symbols overlap in the time domain. Each FBMC symbol is composed of  $L$  samples and carries up to  $M$  filtered subcarriers.

The OQAM modulation consists of separately transmitting the real and imaginary part of a QAM complex symbol to the symbol half-period so that the transmitted symbols are real.

FBMC modulation differs from OFDM modulation in the following aspects:

- IFFT / FFT modules of OFDM are replaced by synthesis and analysis filter banks
- Cyclic prefix insertion is not required for FBMC modulation.
- For FBMC modulation, each sub-channel is filtered separately.
- The prototype function of the OFDM modulation is a rectangular filtering, equal to the inverse of the spacing between the sub-carriers to ensure the orthogonality. On the other hand, the FBMC modulation can benefit from a wide choice of prototype filter to which a polyphase structure can be applied.

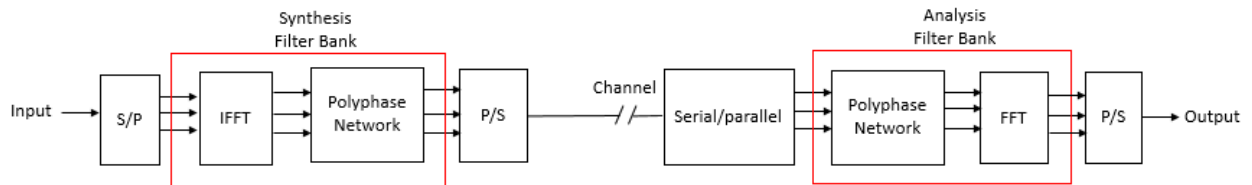


Fig -4: Block Diagram of FBMC-OQAM Transmission System

### 1.3 Block diagram of UFMC modulation

UFMC groups the sub-carriers into sub-bands so that filtering can be applied separately to each sub-band. The transmission chain of a UFMC system is similar to that of an OFDM system. However, for UFMC modulation the filters are placed directly after the IDFT modules, while for the OFDM modulation the filtering operation is performed after the insertion of the cyclic prefix. [8]

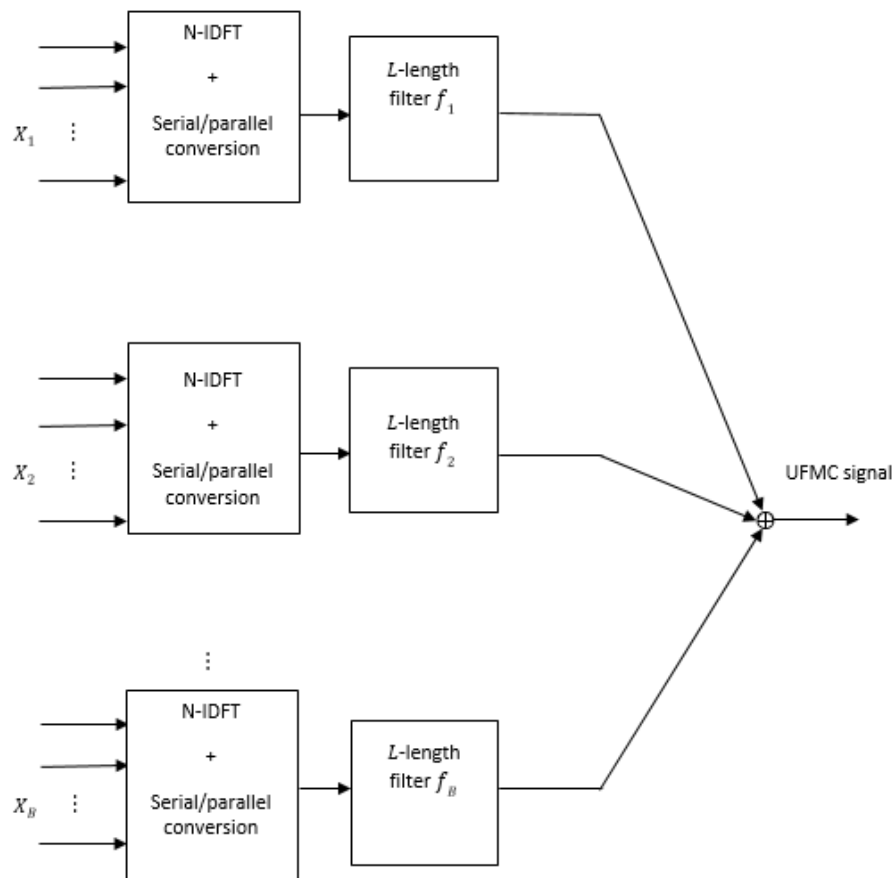


Fig -5: Block Diagram of the UFMC transmitter

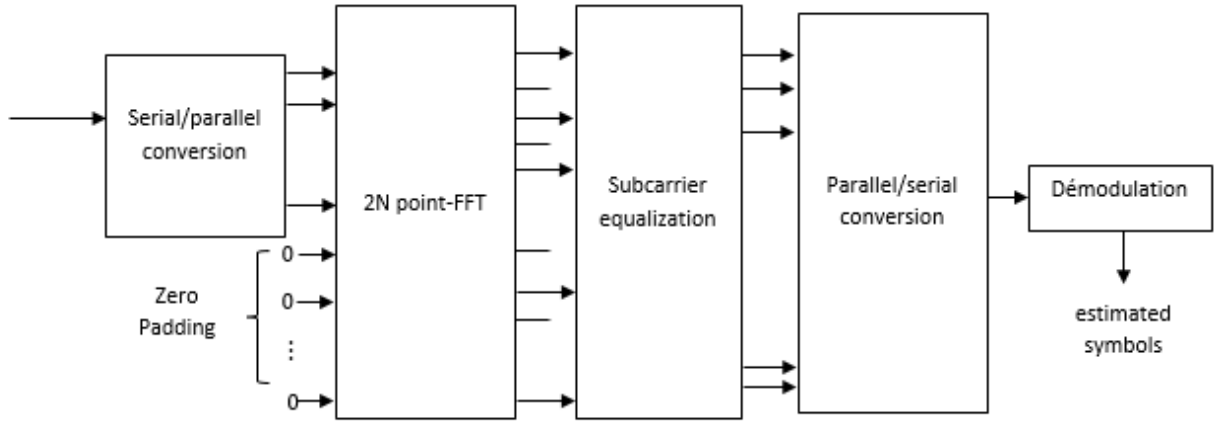


Fig -6: Block diagram of the UFMC receiver

**2. Performance of FBMC-OQAM modulation**

The 5G networks will have to be able to bring new functionalities that would imply an adaptability in the choice of parameters as well as a flexible time-frequency grid.

The radio resource block and corresponds to the minimum time / frequency allocation supported by the network. For 4G networks, an RB (Resource Block) is equivalent to a transmission of 1 ms (14 symbols in time) for 12 sub-carriers spaced 15 kHz as shown in fig-8.

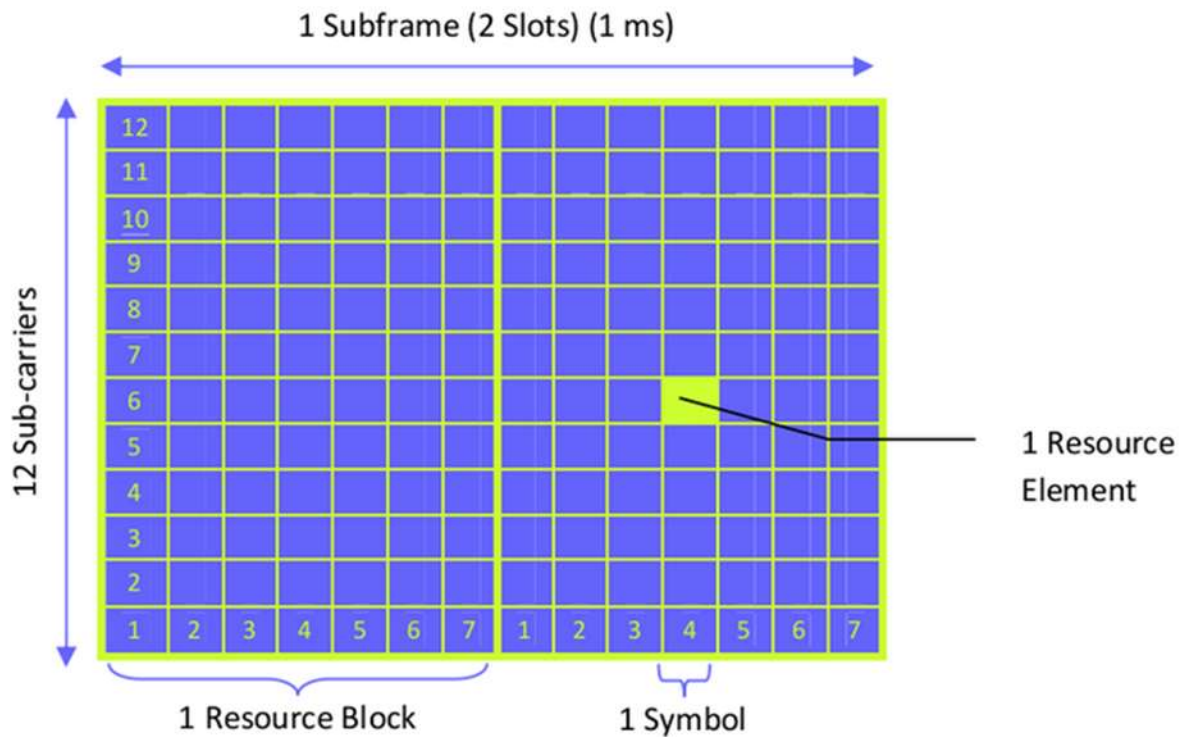
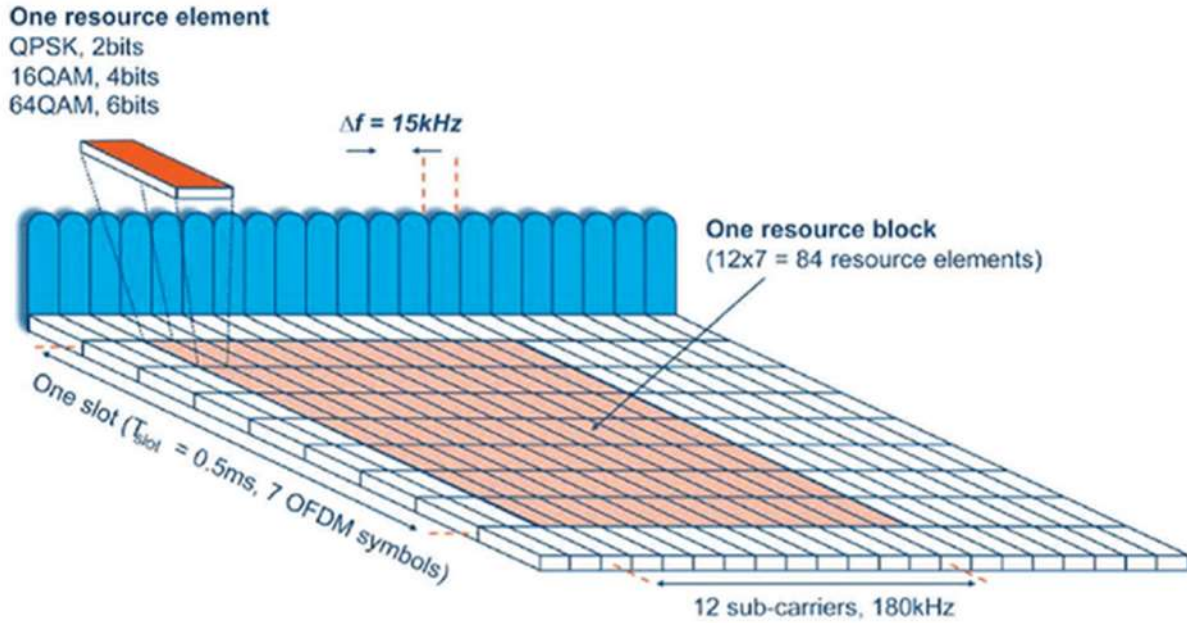


Fig -7: Resource Block of 4G network





**Fig -8:** Time / frequency allocation supported by the 4G network

For current 4G LTE wireless technology, the sub-carrier spacing is set at 15 KHz, regardless of carrier frequency and channel conditions. This approach is not appropriate for 5G that operates over a wide range of spectrum. Indeed, for the case of uRLLC services which requires extremely low latency, it is necessary to shorten the transmission time. This would involve reducing the symbol time, which would require increasing the spacing between the subcarriers.

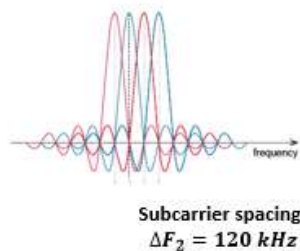
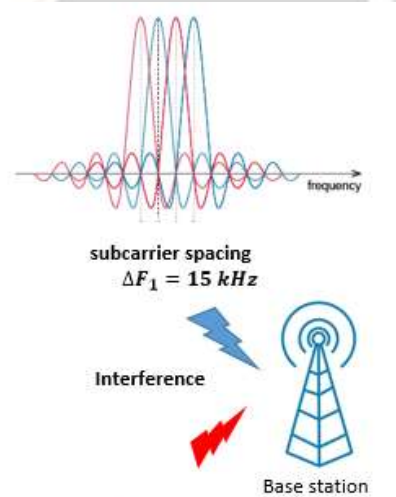


**Fig -9:** MBB service (Mobile BroadBand) and Mission Critical Communications (MCC) service transmitting data in the same band

### 2.1 Signal-to-interference ratio for different use cases

In this simulation, we will calculate the signal interference ratio in the context where two users share the same bandwidth. In this view, it is assumed that both users use different subcarrier spacing (15 kHz and 120 kHz) to account for different channel conditions or different specific user needs.

The objectives of this simulation are:

- Highlight the impact of the guard interval on the signal-to-interference ratio of the FBMC, UFMC and WOLA multicarrier modulations.
- To measure the capacity of the FBMC modulation to take in several cases of use of the same bandwidth.
- Show the adaptability of FBMC-OQAM modulations for low latency transmissions

To calculate the total SIR for 2 users using the same bandwidth, the following expression was used: [5]

$$SIR_{total} = \frac{L_1 K_1 + L_2 K_2}{\|\Re\{G_1^H G_2\}\|_F^2 + \|\Re\{G_2^H G_1\}\|_F^2} \tag{1}$$

Such as  $\|\cdot\|_F$  is the Frobenius norm.

For the case of the CP-OFDM, WOLA, UFMC and F-OFDM modulations, we place ourselves in the complex domain, which will lead to the deletion of the real part of the expression (1).

To calculate the time-frequency efficiency, the following expression was used: [5]

$$\rho = \frac{KL}{(KT+T_G)(FL+F_G)} \tag{2}$$

Such as  $F_G$  represents the required guard band,  $T_G$  required guard time,  $K$  gives the number of symbols transmitted per period,  $T$  and  $F$  correspond respectively to the period and the frequency,  $L$  is the number of subcarriers.

We place ourselves in the case of  $K \rightarrow \infty$  and  $L \rightarrow \infty$ , so that the time-frequency efficiency depends on the density of the symbols  $= 1/TF$ . The density  $\rho = 1 / TF$  makes it possible to measure the spectral efficiency whose theoretical maximum value is equal to 1.

Table-1 shows the characteristics of users sharing the same bandwidth.

**Table -1:** Parameters for the evaluation of the signal-to-interference ratio of the system

Characteristics	User 1	User Scenario 1	User Scenario 2
Transmission matrix	$G_1$	$G_2$	$G_2$
Number of subcarriers used	$L_1 = 96$	$L_2 = 12$	$L_2 = 3$
Number of symbols per block	$K_1 = 9$	$K_2 = 72$	$K_2 = 18$
Spacing between subcarriers	$F_1 = 15$ kHz	$F_2 = 120$ kHz	$F_2 = 480$ kHz
Bandwidth used (MHz)	$F_1 \times L_1 = 1.44$	$F_2 \times L_2 = 1.44$	$F_2 \times L_2 = 1.44$
Time-frequency spacing	$T_1 F_1 = 1.09$	$T_2 F_2 = 1.27$	$T_2 F_2 = 1$

The matrices  $G_1$  and  $G_2$  are similar but the matrix  $G_2$  is shifted in frequency by  $F_1 L_1 + F_G$ . To reduce the out-of-band emissions, we increase the time-frequency spacing, that's why we took  $T_2 F_2 = 1.27$ .

The simulation will consider three scenarios and each scenario will calculate the signal-to-interference ratio  $SIR_{total}$  for two users sharing the same bandwidth. It is known that a flexible configuration of the spacing between subcarriers makes it possible to support several cases of use of the 5G networks. The purpose of the simulation is therefore to determine if the FBMC-OQAM modulation could support multiple bandwidth configurations.

- The first scenario calculates the  $SIR_{total}$  for two users using the F-OFDM, UFMC and WOLA multicarrier modulations to transmit the data symbols where  $T_1F_1 = 1.09$  and  $T_2F_2 = 1.27$  such as  $F_1 = 15$  kHz and  $F_2 = 120$  kHz.
- The second scenario calculates only the  $SIR_{total}$  for two users using the FBMC-OQAM modulation to transmit the information. Since it is accepted that the FBMC-OQAM modulation has the most optimal spectral efficiency, we will take as parameters  $T_1F_1 = 1$  and  $T_2F_2 = 1$  such as  $F_1 = 15$  kHz and  $F_2 = 480$  kHz.
- The third scenario gives the  $SIR_{total}$  for two users using the CP-OFDM modulation. We take  $T_1F_1 = 1.07$  and  $T_2F_2 = 1.07$  such as  $F_1 = 15$  kHz and  $F_2 = 120$  kHz.

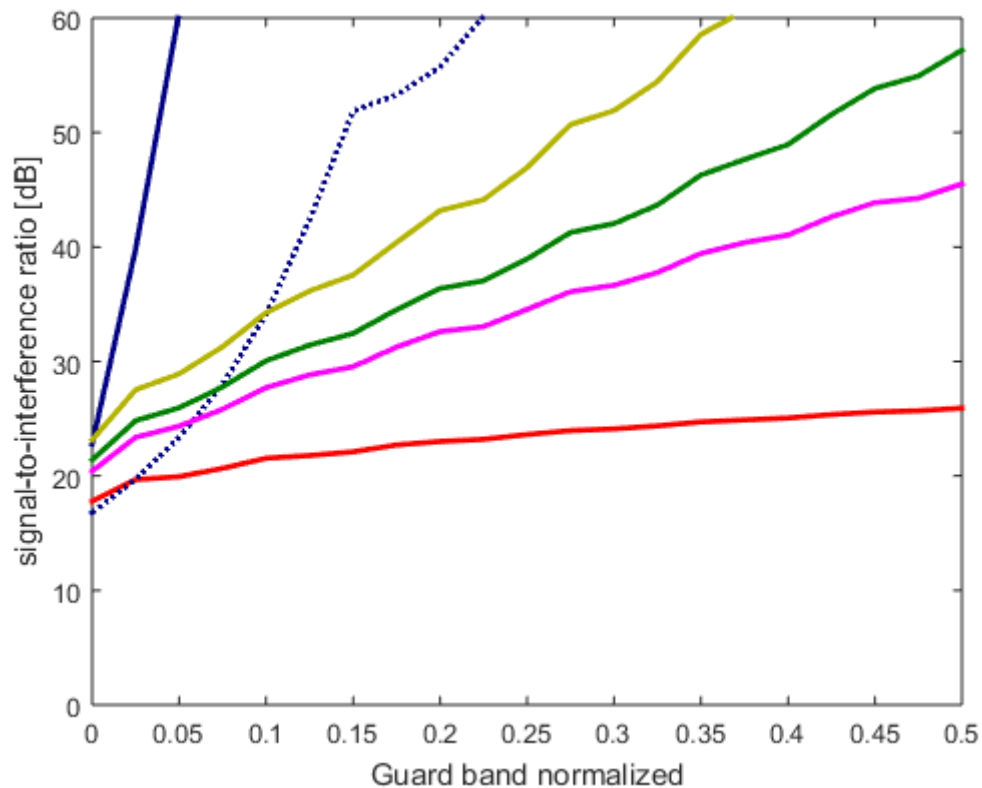


**Fig -10:** SIR performance for different multicarrier modulations

Interpretation of Fig-10:

- vertical axis: guard band normalized  $F_G/FL$
- horizontal axis: signal-to-interference ratio [dB]

First scenario:

- $SIR_{total}$  for two users using F-OFDM modulation to transmit data such as  $F_1 = 15$  kHz and  $F_2 = 120$  kHz:
- $SIR_{total}$  for two users using UFMC modulation to transmit data such as  $F_1 = 15$  kHz and  $F_2 = 120$  kHz:
- $SIR_{total}$  for two users using WOLA modulation to transmit data such as  $F_1 = 15$  kHz and  $F_2 = 120$  kHz:

Second scenario:



- $SIR_{total}$  for two users using FBMC-OQAM modulation to transmit data such as  $F_1 = 15$  kHz and  $F_2 = 120$  kHz:
- $SIR_{total}$  for two users using FBMC-OQAM modulation to transmit data such as  $F_1 = 15$  kHz and  $F_2 = 480$  kHz :

Third scenario:  $SIR_{total}$  for two users using CP-OFDM modulation to transmit data such as  $F_1 = 15$  kHz and  $F_2 = 120$  kHz:

The results of the simulation make it possible to draw the following conclusions:

- The higher the guard band, the less interference is observed.
- The F-OFDM, UFMC and WOLA modulations improve the SIR performance of CP-OFDM modulation. However, these three modulations do not outperform the SIR performance of the FBMC-OQAM modulation whose SIR is high.
- FBMC-OQAM modulation has a higher SIR than CP-OFDM modulation.

A low latency transmission results in a low transmission time. In other words, the symbol duration is shortened, which implies that the spacing between subcarriers is increased. To corroborate our hypothesis about the ability of FBMC-OQAM modulation to support low latency communications, different configurations including multiple values of subcarrier spacing were considered. The simulation results show that the CP-OFDM modulation has the lowest SIR and that the FBMC-OQAM modulation has the highest SIR and surpasses the SIR performance of the other modulations studied (F-OFDM, UFMC and WOLA). Thus, FBMC-OQAM modulation is least sensitive to interference when two users share the same bandwidth.

### 2.2 Optimization of the FBMC-OQAM modulation by the precoding technique

The SC-FDMA multiple access transmission system distributes the signal over a large number of subcarriers while imposing a frequency difference between the carriers equal to the frequency of the symbols in order to guarantee the orthogonality of the subcarriers.

The addition of the "DFT" module makes it possible to obtain a relatively low PAPR compared to the OFDMA technique. Indeed, this precoding block makes it possible to "smooth" the power of the emitted signal and to bring it closer to the effective value of the signal, hence the reduction of the amplitude variations at high frequency.

Fig-11 illustrates the block diagram of the OFDMA and SC-FDMA access techniques used respectively in downlink and uplink by current LTE systems.

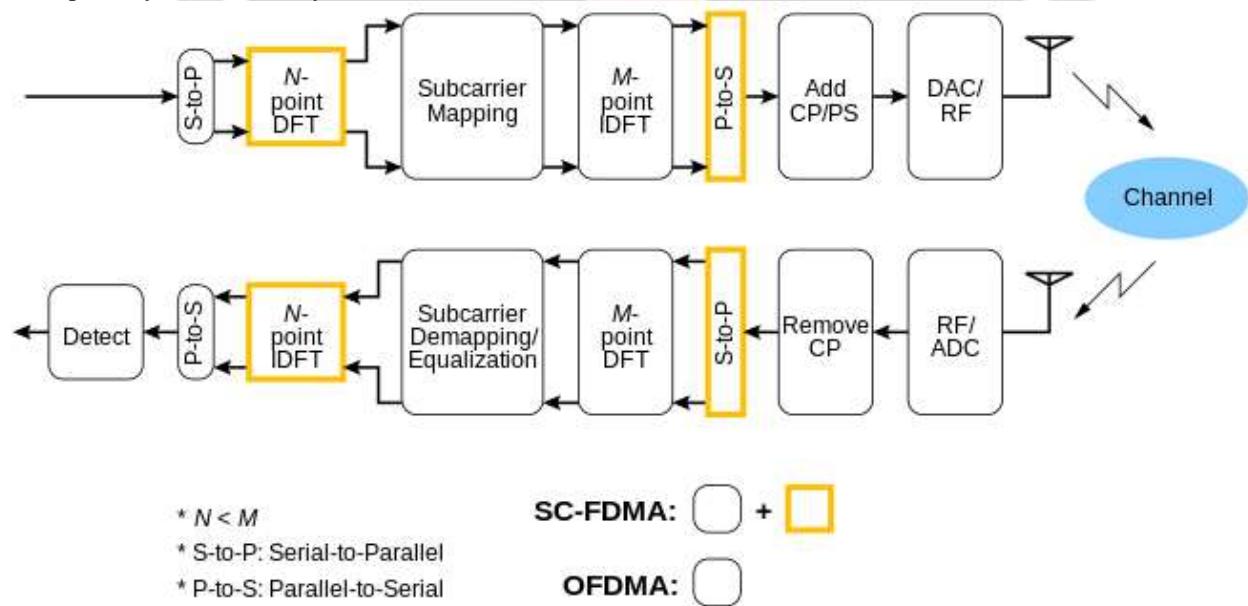


Fig -11: Block diagram of the SC-FDMA access technique

In this part, we plan to precode the FBMC-OQAM modulation by the DFT matrix in order to restore the complex orthogonality of the system. The purpose of the simulation is to propose precoded FBMC-OQAM modulation as an uplink access technique to replace the SC-FDMA technique used by 4G.

Precoding is a technique that restores the complex orthogonality of FBMC-OQAM modulation by using a smaller DFT precoding matrix than that used by the SC-FDMA access technique. [9]

In FBMC-OQAM systems, each time-frequency position can only carry real symbols, so we need 2 time slots to transmit 1 complex symbol. Real-valued symbols are transmitted on a rectangular time-frequency grid, favoring the appearance of intrinsic interference.

Unlike conventional FBMC modulation, the data symbols for the case of the precoded FBMC-OQAM modulation no longer belong to a certain time-frequency position, but are distributed over several temporal or frequency positions in order to restore the complex orthogonality in a block. [10]

The Pruned DFT Spread system is characterized by the restoration of the complex orthogonality of the system via the precoding matrix  $\mathbf{W}$ , which allows data to be spread in the time domain and by the use of a truncated Hermite prototype filter.

The mathematical expression of the transmitted signal  $s(t)$  is expressed as follows:

$$s(t) = \sum_{k=1}^K \sum_{l=1}^L g_{l,k}(t)x_{l,k} \tag{3}$$

The symbol  $x_{l,k}$  of the alphabet  $\chi$  is a symbol derived from a QAM constellation and transmitted to the  $l$ th subcarrier and the  $k$ th temporal position.

The transmitted base pulse  $g_{l,k}(t)$  is a time and frequency offset version of the prototype filter  $p_{TX}(t)$  defined by the following expression:

$$g_{l,k}(t) = p_{TX}(t - kT)e^{j2\pi lF(t-kT)}e^{j\theta_{l,k}} \tag{4}$$

Where  $T$  is the time spacing and  $F$  is the spacing between subcarriers.

After transmission of the signal on an AWGN channel, the received symbols are decoded by projecting the received signal  $r(t)$  on the reception base pulses  $q_{l,k}(t)$ :

$$y_{l,k} = \langle r(t), q_{l,k}(t) \rangle = \int_{-\infty}^{+\infty} r(t)q_{l,k}^*(t)dt \tag{5}$$

The expression of the reception basic pulse  $q_{l,k}(t)$  is given by:

$$q_{l,k}(t) = p_{RX}(t - kT)e^{j2\pi lF(t-kT)}e^{j\theta_{l,k}} \tag{6}$$

The transmission matrix  $\mathbf{G} \in \mathbb{C}^{N \times LK}$  is expressed as follows:

$$\mathbf{G} = [g_{1,1} \quad \dots \quad g_{L,1} \quad g_{1,2} \quad \dots \quad g_{L,K}] \tag{7}$$

Where  $L$  is the number of subcarriers and  $K$  is the number of symbols transmitted for a given period.

The transmitted symbol vector  $\mathbf{x} \in \mathbb{C}^{LK \times 1}$  which groups all the transmitted data symbols is given by:

$$\mathbf{x} = \text{vec} \left\{ \begin{bmatrix} x_{1,1} & \dots & x_{1,K} \\ \vdots & \ddots & \vdots \\ x_{L,1} & \dots & x_{L,K} \end{bmatrix} \right\} = [x_{1,1} \quad \dots \quad x_{L,1} \quad x_{1,2} \quad \dots \quad x_{L,K}]^T \tag{8}$$

In matrix form, the transmission signal can be modeled by the following expression:

$$\mathbf{s} = \sum_{k=1}^K \mathbf{G}_k \mathbf{x}_k = \mathbf{G} \mathbf{x} \tag{9}$$

With  $\mathbf{G}_k \in \mathbb{C}^{N \times L}$  such as  $\mathbf{G}_k = [g_{1,k} \quad \dots \quad g_{L,k}]$  and  $\mathbf{x}_k = [x_{1,k} \quad \dots \quad x_{L,k}]^T \in \mathbb{C}^{L \times 1}$ .

The reception matrix  $\mathbf{Q} \in \mathbb{C}^{N \times LK}$  is expressed as follows:

$$Q = [q_{1,1} \quad \dots \quad q_{L,1} \quad q_{1,2} \quad \dots \quad q_{L,K}] \tag{10}$$

To model a time-varying channel undergoing the effects of multiple paths, an impulse response  $h[m_\tau, n]$  is used where  $n$  is the time position and  $m_\tau$  is the delay.

To express the impulse response, a time varying  $H \in \mathbb{C}^{N \times N}$  convolution matrix defined by:

$$[H]_{i,j} = h[i - j, i] \tag{11}$$

Finally, we get the following expression:

$$y = Q^H r = Q^H H G x + n \tag{12}$$

Where  $r \in \mathbb{C}^{N \times 1}$  represents the sampled received signal and  $n \sim \mathcal{CN}(0, P_n, Q^H Q)$  represents the additive Gaussian white noise such that  $P_n$  is the power of Gaussian white noise in the time domain.

The interference induced by the channel is negligible compared to the noise, which means that the non-diagonal elements of  $Q^H H$  are so small that they are dominated by the noise from which we can deduce the following expression:

$$y \approx \text{diag}\{h\} Q^H G x + n \tag{13}$$

The precoded FBMC-OQAM modulation is characterized by the restoration of the complex orthogonality of the system via the precoding matrix  $\tilde{W}$  which makes it possible to spread the data in the time domain and by the use of a truncated Hermite prototype filter. To do this, the  $L/2$  complex data symbols  $\tilde{x}_k \in \mathbb{C}^{\frac{L}{2} \times 1}$  are distributed on  $L$  subcarriers thanks to the precoding matrix  $C_f$ .

The FBMC symbols transmitted at the time position  $k$  are expressed as follows:

$$x_k = C_f \tilde{x}_k \tag{14}$$

Where  $C_f \in \mathbb{C}^{L \times \frac{L}{2}}$  represents the spreading matrix.

The Spreading operation and the Despreading operation are performed by a DFT matrix denoted  $W \in \mathbb{C}^{L \times L}$ .

We consider the auxiliary vector  $a = \text{diag}\{W^H Q_k^H G_k W\}$  such that  $a \in \mathbb{R}^{L \times 1}$ .

The precoding matrix can be modeled as follows:

$$C_f = \tilde{W} \text{diag}\{\tilde{b}\} \tag{15}$$

Where  $\tilde{W} \in \mathbb{C}^{L \times \frac{L}{2}}$  which corresponds to the DFT matrix defined by  $\tilde{W} = W \begin{bmatrix} I_{\frac{L}{2}} \\ \mathbf{0}_L \end{bmatrix}$  and  $\tilde{b} \in \mathbb{R}^{\frac{L}{2} \times 1}$  is a scale

factor defined by  $[\tilde{b}]_i = \sqrt{\frac{1}{[a]_i}}$  such as  $i = 1, 2, \dots, \frac{L}{2}$ .

The element  $[a]_i$  corresponds to the  $i$ th column vector of  $W$ .

So, the Pruned DFT Spread FBMC technique then consists in using a precoding matrix  $C_f$  to reduce the size of the DFT, so that only the column vectors of  $W$  corresponding to the  $\frac{L}{2}$  largest elements of  $a$  are used (only the first  $\frac{L}{2}$  vectors of  $W$ ).

The truncated Hermite prototype filter is used by the system: it is a prototype Hermite filter for which the pulse is set to zero after the first zero crossing.

The received data symbols  $\tilde{y}_k \in \mathbb{C}^{\frac{L}{2} \times 1}$  are obtained by a simple equalization of the received symbols  $e_k \in \mathbb{C}^{L \times 1}$  such that:

$$\tilde{y}_k = C_f^H \text{diag}\{e_k\}^{-1} y_k \tag{16}$$

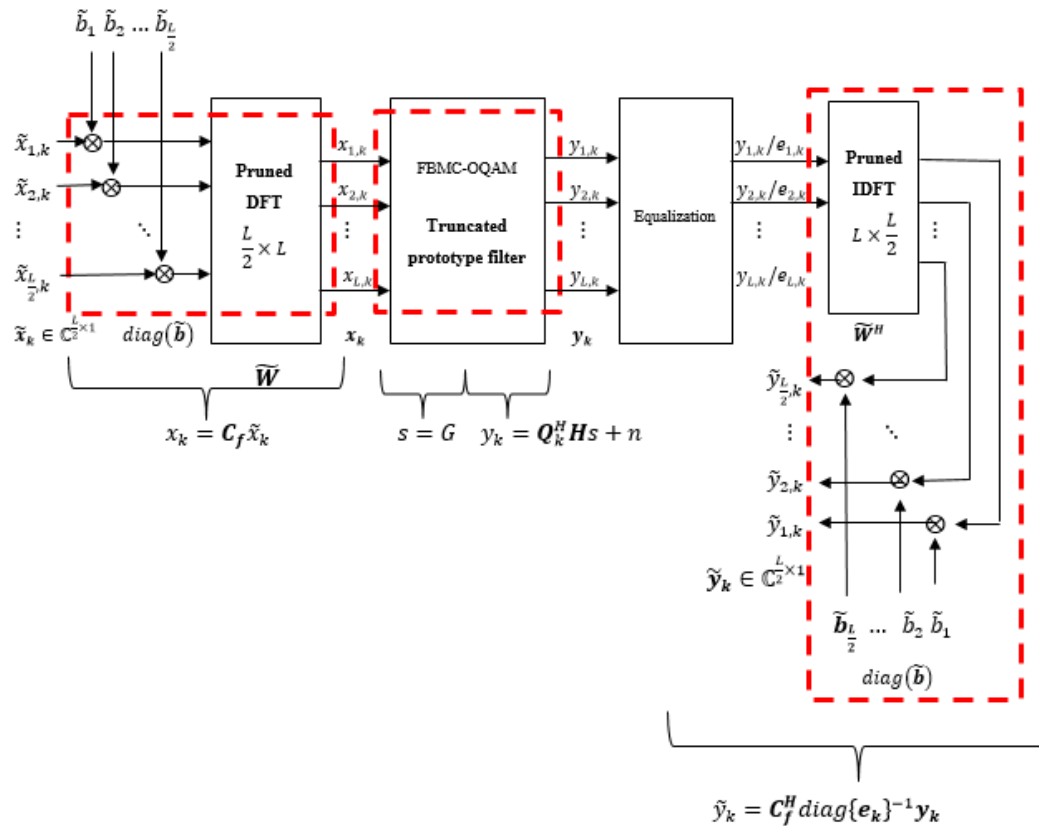


Fig -12: Block diagram of the Pruned DFT Spread FBMC technique

To evaluate the PAPR of a given system, the complementary cumulative distribution function (CCDF) used to search for the probability that a variable takes a value greater than  $x$  is used.

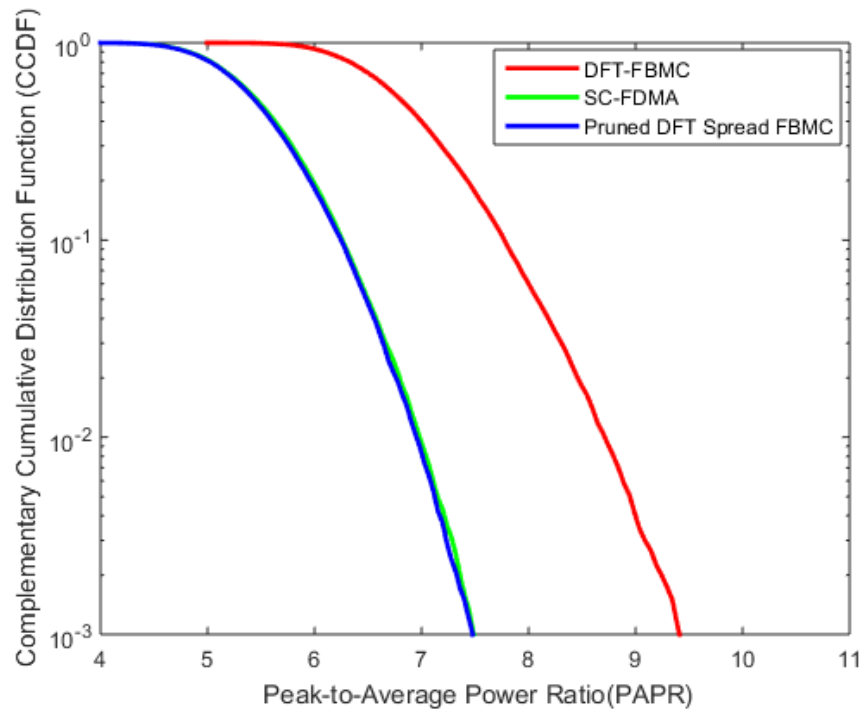
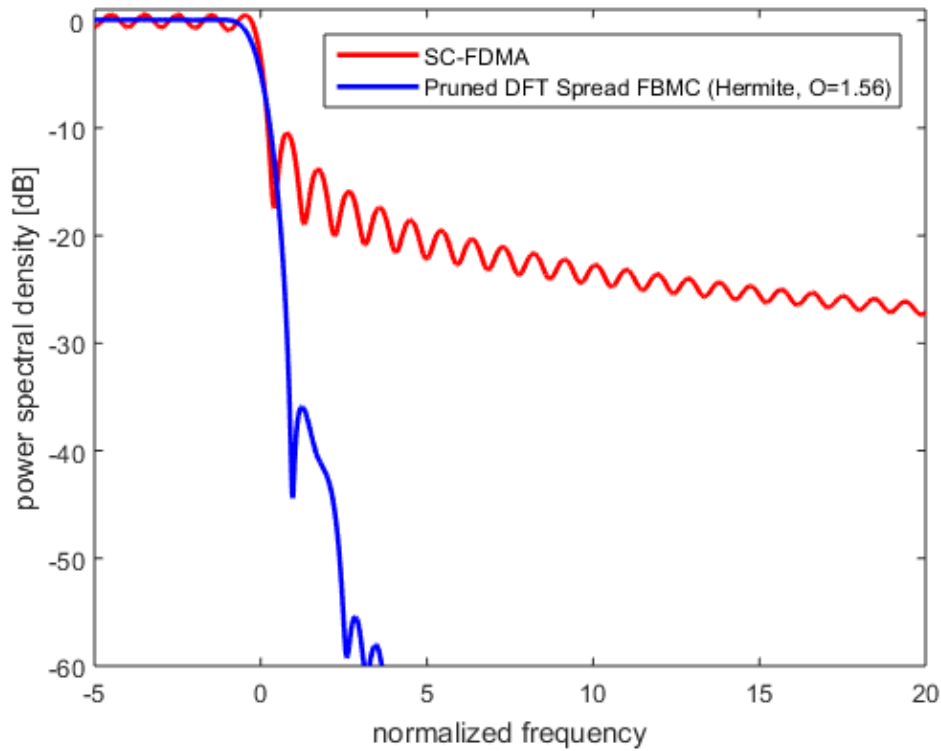
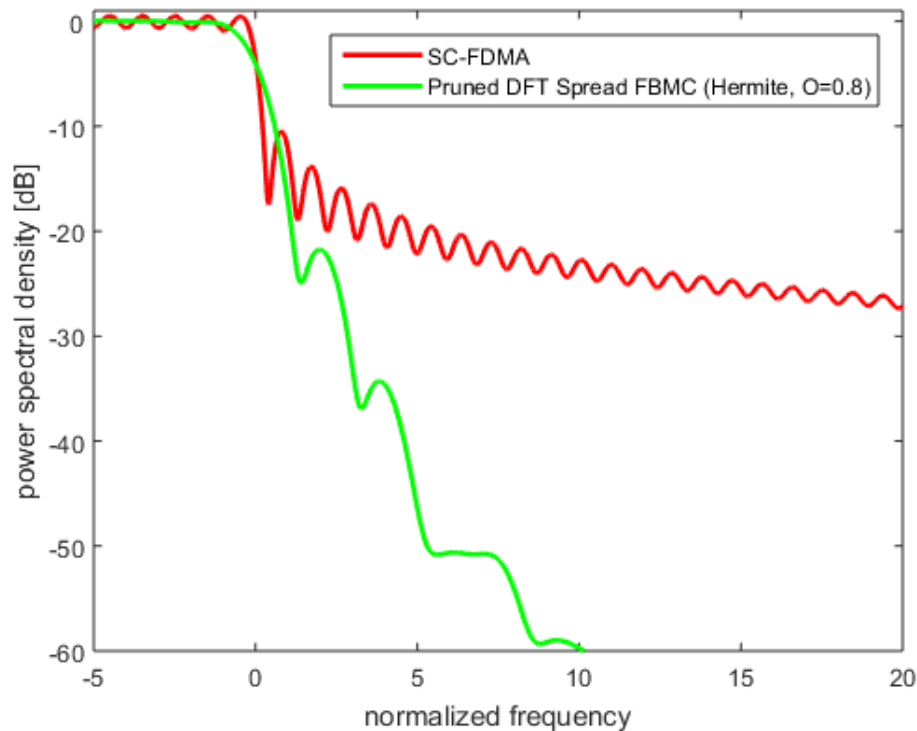


Fig -13: PAPR techniques SC-FDMA, DFT-FBMC and Pruned DFT Spread FBMC

Fig-13 shows that the DFT-FBMC technique has the highest PAPR among the three access techniques studied. The Pruned DFT Spread technique has the same PAPR as the SC-FDMA access technique. Thus, by having a low PAPR, the Pruned DFT Spread FBMC technique makes it possible to meet the needs of 5G networks in terms of energy efficiency.



**Fig -14:** Power spectral density of SC-FDMA and Pruned Spread FBMC techniques with overlap factor  $O = 1.56$



**Fig -15:** Power spectral density of SC-FDMA and Pruned Spread FBMC techniques with overlap factor  $O = 0.8$



From figures 14 and 15, the choice of the value of the overlap factor is essential. In fact, by decreasing the overlap factor ( $O = 0.8$  in fig-14 against  $O = 1.56$  in fig-15), out-of-band emissions are increased. In other words, the more one increases the value of the overlap factor, the more the out-of-band emissions decrease. Fig-16 shows that the spectral properties of the Pruned DFT Spread FBMC and FBMC-OQAM techniques are similar.

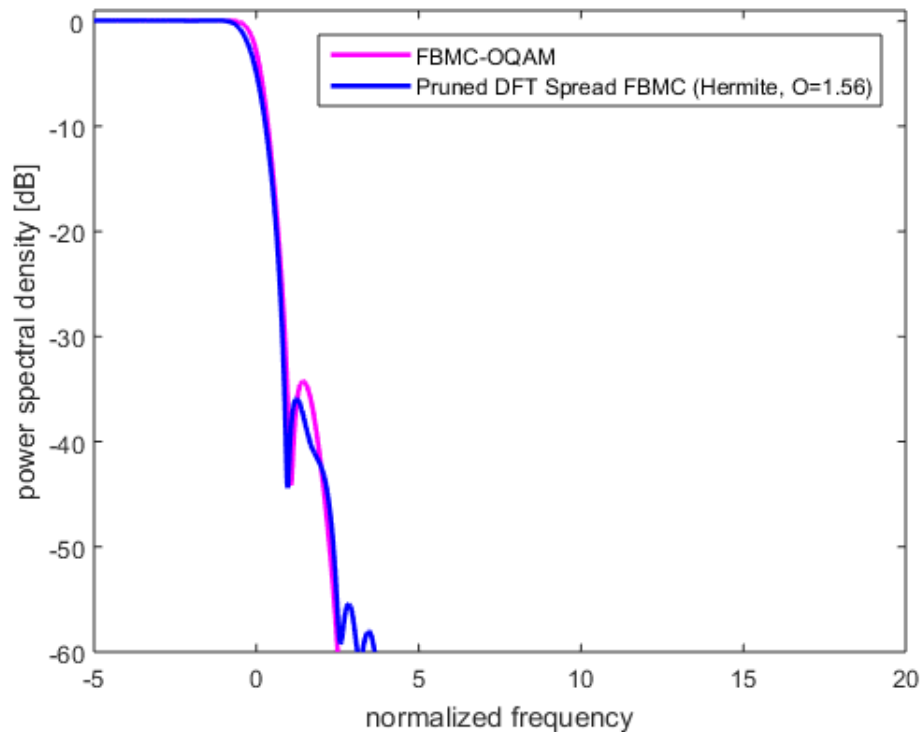


**Fig -16:** Power spectral density of FBMC-OQAM and Pruned Spread FBMC techniques with overlap factor  $O = 1.56$

### 3. CONCLUSIONS

FBMC-OQAM molding is highly qualified to support the different use cases of 5G. Indeed, our theoretical hypothesis is validated by the simulations that have been implemented and which consist in measuring the interference of a transmission system for which several users with different needs use the same bandwidth. From this analysis, it appears on the one hand that the FBMC-OQAM modulation is more efficient in terms of SIR than the WOLA, UFMC and F-OFDM modulations and secondly that the CP-OFDM modulation is the least efficient.

To reduce PAPR, LTE systems use the uplink SC-FDMA access technique. However, the DFT precoding block used by the SC-FDMA technique is not adapted to the FBMC technique, which is why the Pruned DFT Spread FBMC technique has been proposed in order to combine the advantages brought by the OFDM-OQAM modulation and the SC-FDMA access technique.

The Pruned DFT Spread FBMC technique optimizes the spectral and energy efficiencies of the system. In fact, it makes it possible to benefit from a low out-of-band emission comparable to that of the FBMC-OQAM technique and from a low PAPR identical to that of the SC-FDMA technique.

Moreover, the spectral and energy efficiencies are not the only technological criteria to optimize for a better deployment of 5G. That's why our future research will focus on the impact of the overlap factor values and the system latency.

### 6. REFERENCES

- [1]. A. Alexiou, « *5G Wireless Technologies* », the Institution of Engineering and Technology, 2017.
- [2]. X.Ge and W. Zhang, « *5G Green Mobile Communication Networks* », Springer, 2019.
- [3]. P. Marsch, Ö. Bulakçı, O. Queseth and M. Boldi, « *5G System Design Architectural and Functional Considerations and Long Term Research* », Wiley, 2018

- [4]. R. Nissel, « *Symbol detection in high speed channels* », in *The Vienna LTE-Advanced Simulators: Up and Downlink, Link and System Level Simulation*, pp. 39–60, Singapore: Springer-Verlag, 2016.
- [5]. C. L  l  , P. Siohan, R. Legouable and M. Bellanger, « *OFDM/OQAM for spread spectrum transmission* », in *Proceedings of the International Workshop on Multi-Carrier Spread-Spectrum (MCSS '07)*, Herrsching, Germany, May 2007.
- [6]. X. Wang, « *Cellular architecture and key technologies for 5G wireless communication networks* », *IEEE Commun. Mag.* 52(2), pp. 122-130, 2014.
- [7]. P. Banelli, S. Buzzi, G. Colavolpe, A. Modenini, F. Rusek and A. Ugolini, « *Modulation formats and waveforms for 5G networks: who will be the heir of OFDM? An overview of alternative modulation schemes for improved spectral efficiency* », *IEEE Signal Processing Magazine*, 31: 80-93, 2014.
- [8]. X. Wang, T. Wild, F. Schaich and A. Fonseca dos Santos, « *Universal filtered multicarrier with leakage-based filter optimization* », *Proceedings of 20th European Wireless Conference*, pp. 1-5, 2014.
- [9]. C. L  l  , P. Siohan, R. Legouable and M. Bellanger, « *CDMA transmission with complex OFDM/OQAM* », *EURASIP Journal on Wireless Communications and Networking*, vol. 2008, Article ID 748063, 12 pages, 2008.
- [10]. R. Nissel, « *Filter bank multicarrier modulation for future wireless systems* », *Dissertation, TU Wien*, 2017.

